# Electronic Supplementary Information (ESI)

**Facile Edge Functionalization of Graphene Layers with a Biosourced 2-Pyrone**

Fatima Margani,[†] Martina Magrograssi,[†] Marco Piccini, Luigi Brambilla, Maurizio Galimberti,* and Vincenzina Barbera*

[1]Politecnico di Milano, Department of Chemistry, Materials and Chemical Engineering "G. Natta", Via Mancinelli 7, 20131 Milano, Italy

*Corresponding authors.
Maurizio Galimberti − Department of Chemistry, Materials and Chemical Engineering "G. Natta", Politecnico di Milano, 20131 Milano, Italy; orcid.org/0000-0001-5770-7208;
Email: maurizio.galimberti@polimi.it

Vincenzina Barbera − Department of Chemistry, Materials and Chemical Engineering "G. Natta", Politecnico di Milano, 20131 Milano, Italy; orcid.org/0000-0002-4503-4250;
Email: vincenzina.barbera@polimi.it

[†] F.M and M.M. contributed equally to the work.

Number of pages: 12
Number of figures:12
Number of tables: 2

## Table of Contents

**S1. Characterization of Pristine HSAG**

*Elemental analysis*

Chemical composition, determined by elemental analysis, was (mass %): carbon 99.5, hydrogen 0.4, nitrogen 0.1, oxygen 0.0. TGA revealed the following mass loss: 3.2% below 700°C. Surface area was determined by BET according to ASTM D6556 method and was found to be 330.3 $m^2/g$. Average size of HSAG particles was evaluated by means of dynamic light scattering, obtaining values representing the hydrodynamic radius of HSAG particles in water dispersions. Average values were 500 nm in the as prepared dispersion and 190 nm after centrifuging the dispersion for 30 min centrifugation at 9000 rpm. Transmission electron micrograph taken on supernatant suspension after 60 min centrifugation at 9000 rpm revealed graphite stacks randomly arranged, with lateral size between about 300 nm and 500 nm.

*FT-IR spectroscopy*

Functional groups on pristine HSAG were detected by analysing the samples in a Diamond Anvil Cell (DAC). FT-IR spectrum of HSAG is reported in **Figure S1**.

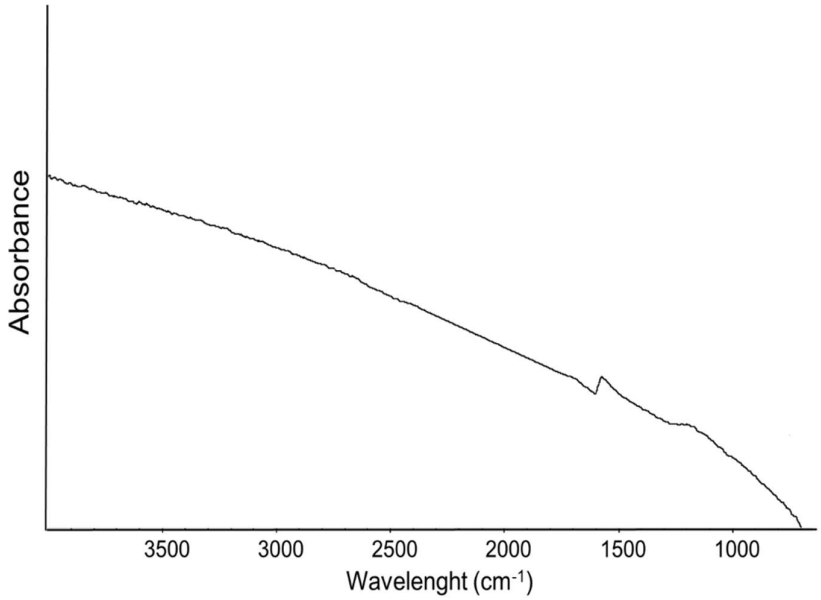


**Figure S1.** FT-IR spectrum of HSAG

Spectrum of HSAG is characterized by an increasing background toward high wavenumbers due to diffusion/reflection phenomena of the IR light by the particles of the sample. The spectrum is characterized by the feature centered at 1590 $cm^{-1}$ which is the absorption peak of graphite and graphene materials, assigned to $E_{1u}$ IR active mode of collective C=C stretching vibration.

*Raman spectroscopy*

Raman spectroscopy is widely employed for the study of carbonaceous materials. In Raman spectrum, two peaks, named D and G and located at 1350 $cm^{-1}$ and 1590 $cm^{-1}$ respectively, are investigated. The G peak is due to bulk crystalline graphite (graphene), whereas the D peak appears in the presence of either structural defects, such as holes, $sp^3$ or sp carbon atoms, free radicals, distortions from

planarity, grafted functional groups or confinement (e.g. by edges) of the graphitic layers. The Raman spectrum of HSAG (recorded with the laser excitation at 632.8 nm) is reported in **Figure S2.**

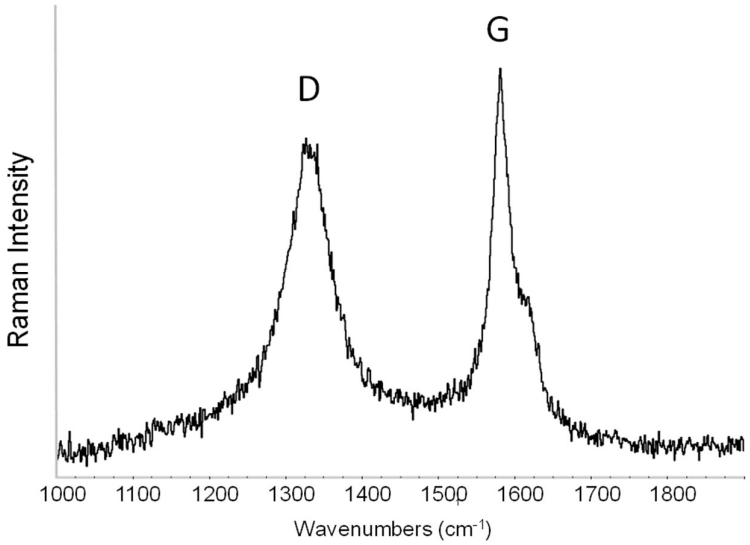


**Figure S2.** Raman spectrum with normalized intensity of HSAG

Analysis was performed on a good number of spots and spectra can be considered representative of the investigated samples. In the spectrum of HSAG the high intensity of the D band can be interpreted taking into account what reported in the literature for Raman spectra of ball milled graphite. The pronounced D band is thus due to the different types of molecular disorder. Raman components between G and D peaks are due to disordered $sp^3$ carbon structures.

*Thermogravimetric analysis*

Thermogravimetric analysis (TGA) was used to quantitatively estimate the degree of functionalization in all adducts. In **Figure S3** thermogram of HSAG is reported.

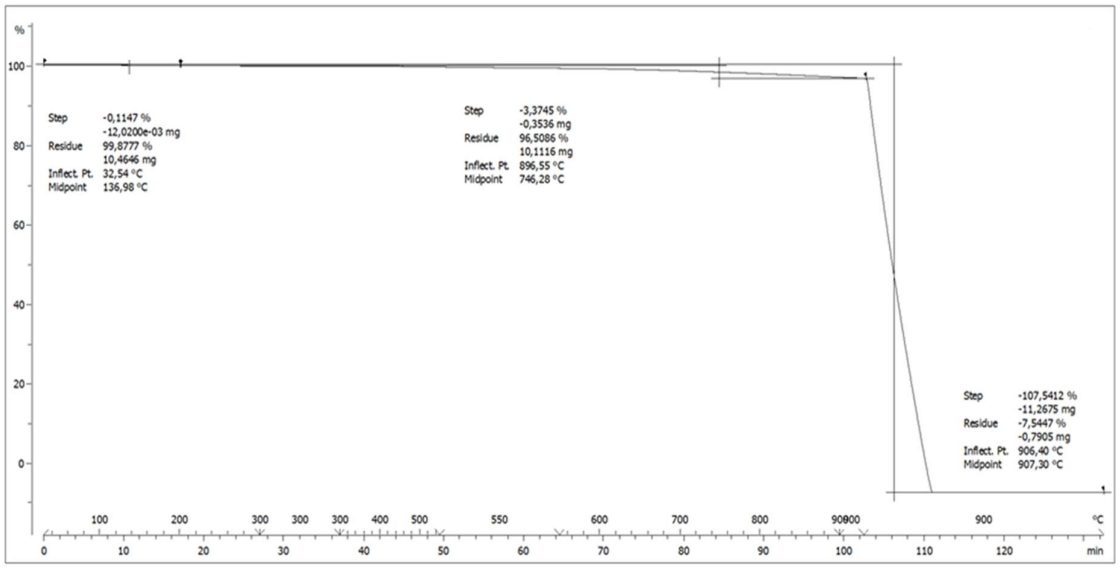


**Figure S3.** TGA thermogram under $N_2$ of HSAG

A three-step decomposition profile can be observed. The first mass loss below 150 °C can be attributed to the water removal. The second and third step, between 150 and 700 °C, are attributed to the decomposition of oxygen-containing groups and removal of alkenyl groups presents as defect in HSAG. At temperature higher than 700 °C the combustion of graphitic carbon occurs. Results are summarized in Table 1 in the text. In general, much larger loss in the range of 150 – 700 °C are detected for functionalized CA with respect to the corresponding pristine CA, as confirmation of the presence of new functional groups.

*High resolution transmission electron microscopy*

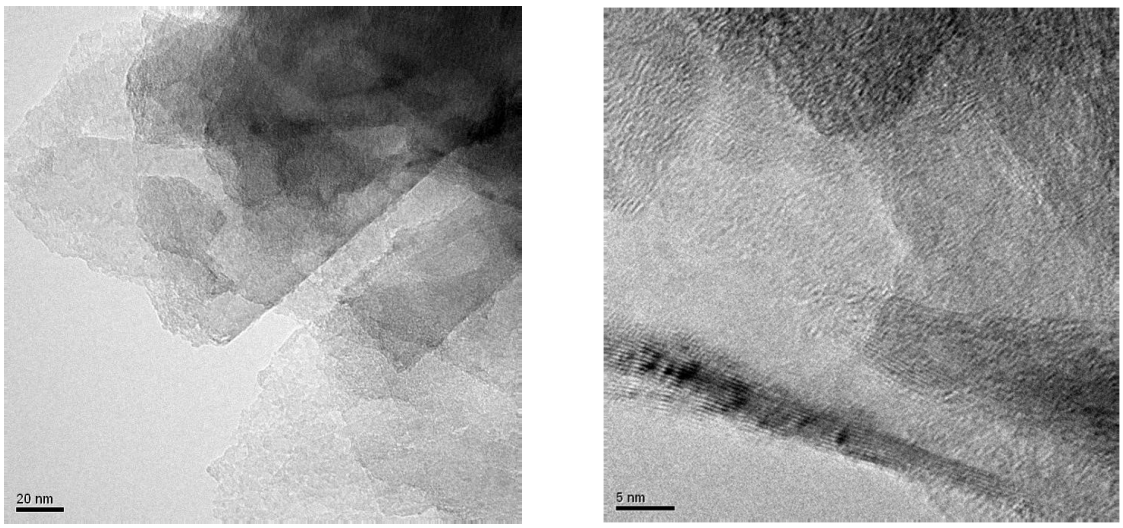


**Figure S4.** HRTEM Micrographs of pristine HSAG, isolated from supernatant suspensions (1 mg/1 ml), after centrifugation for 30 min at 6000 rpm.

**S2. Scale Up for the synthesis of Sodium 3-Scetoxy-2-oxo-2*H*-pyran-6-carboxylate (Pyr-COONa)**

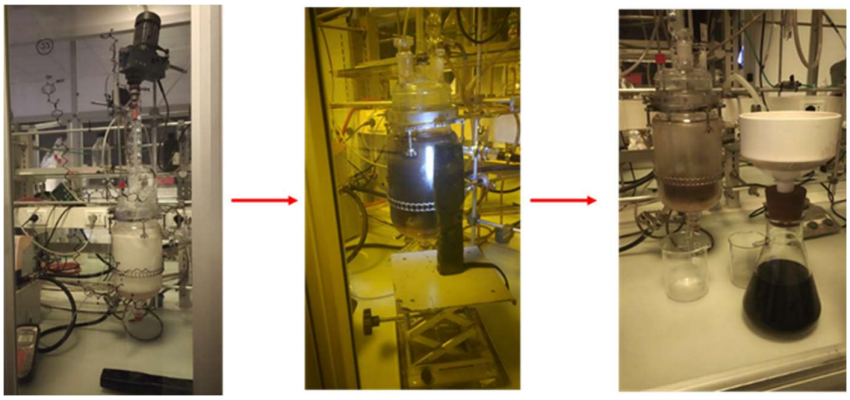

**Figure S5.** Scale up for the synthesis of Sodium 3-Acetoxy-2-oxo-2*H*-pyran-6-carboxylate (Pyr-COONa)

The process (**Figure S5**) was thus performed in the facilities of an Italian company (Materiali Sensibili S.r.l.), a chemical synthesis company located in San Giuliano Milanese (MI), using a 3L glass reactor with external jacket.

**S3. Characterization of HSAG-Pyr-COOEt adduct**

**S 3.1 Characterization Techniques**

$^{1}$H NMR and $^{13}$C NMR spectra were recorded using a 400 MHz (100 MHz $^{13}$C) Bruker NMR spectrometer at 298 K.

Thermogravimetric analysis (TGA) was carried out on a thermal analyzer (Mettler TGA SDTA/851), following the standard method ISO9924-1. Under a $N_2$ flow rate of 60 mL/min, samples (10 ±0.5 mg) were heated from 30 to 300°C at 10°C/min and hold up at 300°C for 10 min. Then, heated up to 550°C with a heating rate of 20°C/min and kept at this temperature for 15 min. Hence, they were further heated up to 900°C at 10°C/min and kept at 900°C for 20 min under flowing air (60 mL/min). Functionalization yields were estimated from TGA data through the following equation (Equation 1).

$$Functionalization\ Yield\ (\%) = \frac{Pyr{-}COOR\ mass\ \%\ in\ \left(HSAG{-}Pyr{-}COOR\ adduct\right)after\ \ acetone\ washi}{Pyr{-}COOR\ mass\ \%\ in\ (HSAG{-}Pyr{-}CO\ \ \ adduct)before\ acetone\ washing} * 100\% \qquad \text{(Eq. 1)}$$

The % mass of Pyr-COOR in HSAG/Pyr-COOR adducts (before and after filtration) was obtained as the mass loss in the range from 150 °C to 700 °C in TGA analysis. Data are shown in Table 1 below in the text.

A ThermoElectron Continuμm IR microscope coupled with a Nicolet Nexus FT-IR spectrometer was used to record Fourier-Transform InfraRed (FT-IR) spectra in transmission mode (128 scan, resolution of 4 $cm^{-1}$) with a diamond anvil cell (DAC).

Raman spectra were collected at room temperature in solid state by using a Horiba Jobin Yvon Labram HR800 dispersive Raman spectrometer coupled with Olympus BX41 microscope equipped with a 50X objective. In order to prevent samples degradation, the He/Ne excitation laser line at 632.8 nm was set at 0.5 mW. Spectra were obtained collecting four acquisitions (30 seconds each) with a spectral resolution of 2 $cm^{-1}$. Each Raman spectrum reported in this work comes from the average of at least 5 spectra, recorded in different points of the samples.

High-resolution transmission electron microscopy *(*HRTEM*)* of HSAG samples was carried out through a Philips CM 200 field emission gun microscope with an accelerating voltage of 200 kV. After sonication, few drops of HSAG water suspensions were placed on 200 mesh lacey carbon-coated copper grid and air-dried before analysis. To avoid structural transformation during acquisition of HRTEM images, short acquisition times and low beam current densities were adopted. The number and the dimensions of stacked layers detectable in HRTEM micrographs was estimated with the Gatan Digital Micrograph software.

The water suspensions of HSAG samples (3 mL) were analyzed in a Hewlett Packard (Palo Alto, CA, USA) 8452A Diode Array Spectrophotometer using a cell quartz with 1 cm optical path in the UV-visible region. All spectra were recorded using water as blank and reported as intensity absorption in function of the wavelength of the radiation between 200 and 750 nm.

Wide-angle X-ray diffraction (WAXD) data were collected on an automatic Bruker D8 Advance diffractometer with nickel filtered Cu–Kα radiation. Patterns were recorded in reflection in 10° – 100° as the 2θ range, being 2θ the peak diffraction angle. The Bragg law was used to calculate the distance between crystallographic planes. The Scherrer equation (equation 2) was applied to determinate the $D_{hk\ell}$ correlation length in the direction perpendicular to the *hkl* crystal graphitic planes:

$$D_{hk\ell} = K\,\lambda / (\beta_{hk\ell} \cos\theta_{hk\ell}) \qquad \text{(Eq. 2)}$$

where: K is the Scherrer constant, λ is the wavelength of the irradiating beam (1.5419 Å, Cu-Kα), $\beta_{hk\ell}$ is the width at half height, and $\theta_{hk\ell}$ is the diffraction angle. The instrumental broadening, $b$, was determined by obtaining a WAXD pattern of a standard silicon powder 325 mesh (99%), under the same experimental conditions. The width at half height, $\beta_{hk\ell} = (B_{hk\ell} - b)$ was corrected for each observed reflection with $\beta_{hk\ell} < 1°$ by subtracting the instrumental broadening of the closest silicon reflection from the experimental width at half height, $B_{hk\ell}$.

### S.3.2 Thermogravimetric analysis

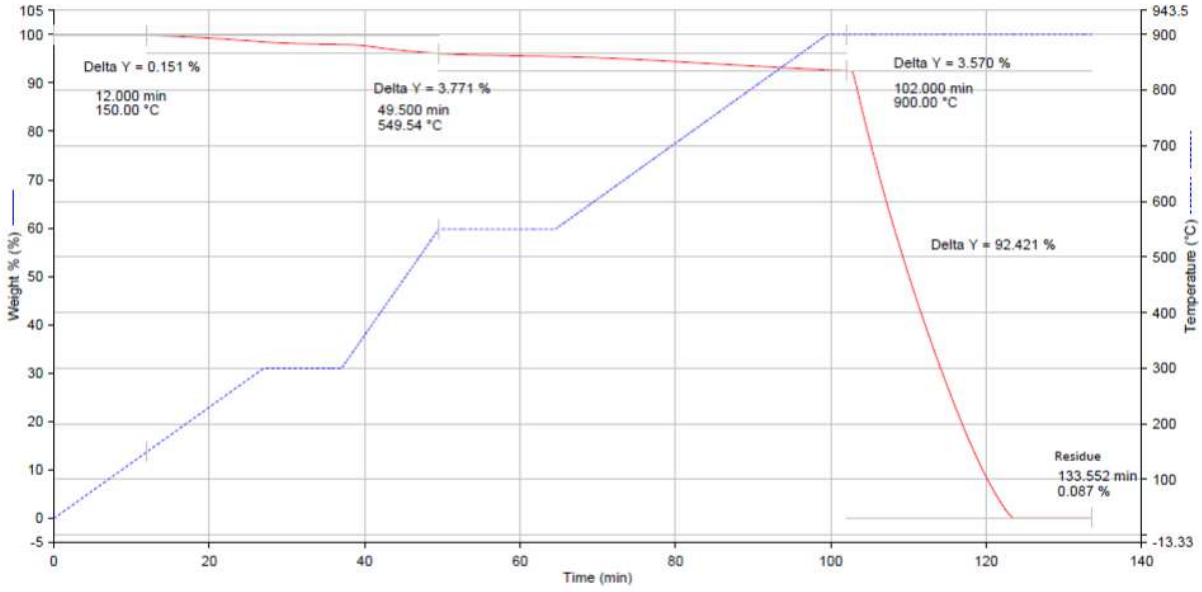


**Figure S6.** Thermogram of HSAG/Pyr-COOEt thermal adduct

TGA analysis (**Figure S6**) was performed as described in the experimental part. Quantitative data of mass losses are in the manuscript.

### S.3.3 Wide-angle X-ray diffraction (WAXD)

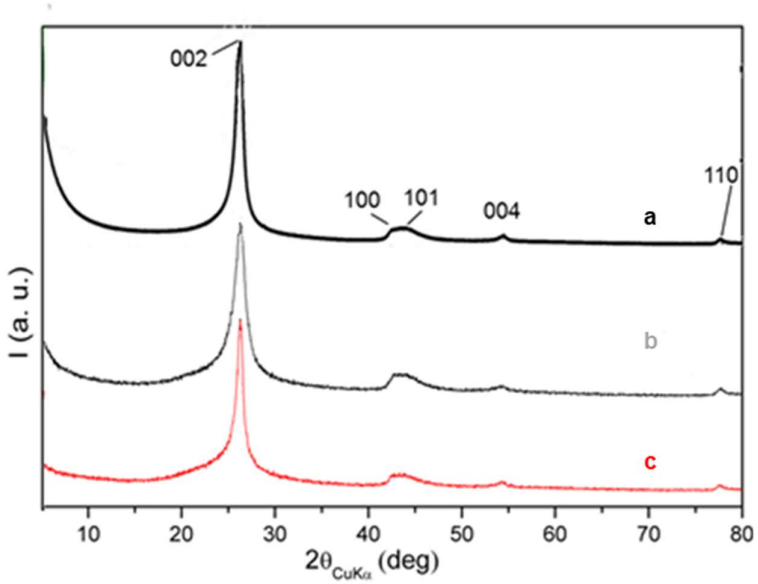


**Figure S7.** WAXD patterns of HSAG (black line), HSAG/ Pyr-COOEt-M (grey line), HSAG/ Pyr-COOEt-T 160°C (red line).

Crystalline order in the direction orthogonal to structural layers in pristine HSAG (**Figure S7**) is detected by two (00ℓ) reflections: 002 at 26.6° (interlayer distance of 0.338 nm) and 004 at 54.3°. The in plane order is shown by 100 and 110 reflections, at 42.5° and 77.6° respectively. From the calculation HSAG/Pyr-COOEt-M and HSAG/ Pyr-COOEt-T 160°C samples show 21 and 31 stacked layers respectively.

This finding supports the occurring of an edge (peripheral) functionalization of graphene layers.

### S.3.4 Estimation of the Hansen Solubility Parameters (HSP) and Hansen Solubility Sphere

In Table S1, dispersion tests were performed, as described in the experimental part, for HSAG and HSAG-Pyr-COOEt in various solvents.

The Hansen solubility parameters of the solvents are in **Table S.1**

**Table S1.** Hansen solubility parameters of the solvents[a,b].

| Solvent | $\delta_D$ | $\delta_P$ | $\delta_H$ | $\delta_T$ [c] |
|---|---|---|---|---|
| Hexane | 14.9 | 0.0 | 0.0 | 14.9 |
| Ethyl acetate | 15.8 | 5.3 | 7.2 | 18.1 |
| Toluene | 18.0 | 1.4 | 2.0 | 18.2 |
| THF | 16.8 | 5.7 | 8.0 | 19.5 |
| 2-propanol | 15.8 | 6.1 | 16.4 | 23.6 |
| Methanol | 15.1 | 12.3 | 22.3 | 29.6 |
| Acetone | 15.5 | 10.4 | 7.0 | 19.9 |
| Water | 18.1 | 17.1 | 16.9 | 30.1 |

[a] Used for the estimation of the solubility parameters
[b] Unit of measurement: $MPa^{1/2}$; [c] $\delta_T^2 = \delta_D^2+\delta_P^2+\delta_H^2$

Results of the visual inspection for HSAG/ Pyr-COOEt are in **Table S.2.**

**Table S2**. Results of inspection of stability of HSAG/ Pyr-COOEt dispersions in various solvents [a,b]

| Solvent | After one hour | After one week |
|---|---|---|
| Hexane | BAD | BAD |
| Ethyl acetate | BAD | BAD |
| Toluene | BAD | BAD |
| THF | BAD | BAD |
| 2-Propanol | BAD | BAD |
| Methanol | GOOD | BAD |
| Acetone | GOOD | GOOD |
| Water | GOOD | BAD |

[a]Concentration: 1 mg/mL; [b] GOOD: homogeneous dispersion. BAD: separation of the black powder from the solvent

The MATLAB algorithm used for the preparation of Hansen's sphere is shown in **Figure S8.**

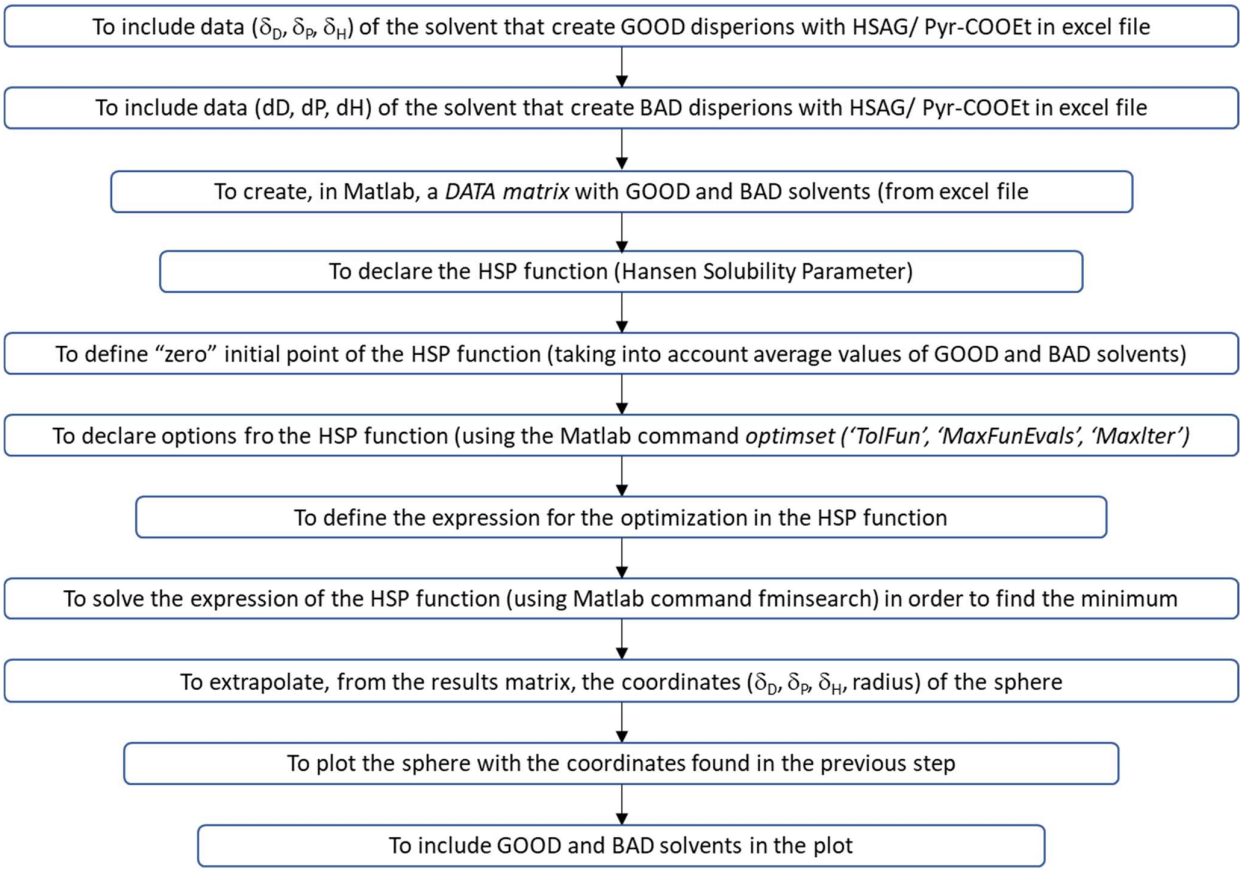


**Figure S8.** MATLAB algorithm used for the preparation of Hansen's sphere

**S 3.5 Water suspensions of HSAG adducts with Pyr-COOEt**

The preparation scheme of water suspensions of HSAG/Pyr-COOEt adducts is resumed in **Figure S9.**

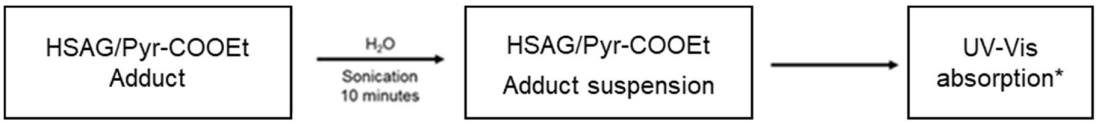


*Uv-vis absorption was measured after 2hours, 5 hours, 24 hours and 7 days

**Figure S9.** Block diagram for the preparation of water suspensions of adducts between HSAG and α-pyrone derivative.

As described in the experimental part, water suspensions of HSAG/Pyr-COOEt adducts at different concentrations (1 mg/mL; 0.5 mg/mL; 0.3 mg/mL; 0.1 mg/mL; 0.05 mg/mL; 0.01 mg/mL; 0.05 mg/mL) were prepared through a mild sonication (**Figure S10**)

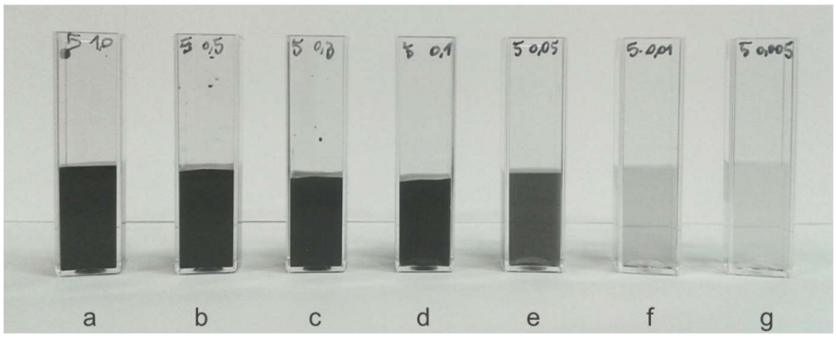


**Figure S10.** Stable water suspensions of HSAG/Pyr-COOEt adduct at different concentration: (1 mg/mL, 0,5 mg/mL, 0,3 mg/mL, 0,1 mg/mL, 0,05 mg/mL, 0,01 mg/mL, 0,005 mg/mL)

UV-Vis absorbance of HSAG/Pyr-COOEt water suspensions at decreasing concentration is shown in **Figure S11**. The absorbance monotonously increases with HSAG/Pyr-COOEt concentration. UV-Vis traces show that it does exist a linear correlation between absorption at 320 nm and adduct concentration above 0,3 mg/mL.

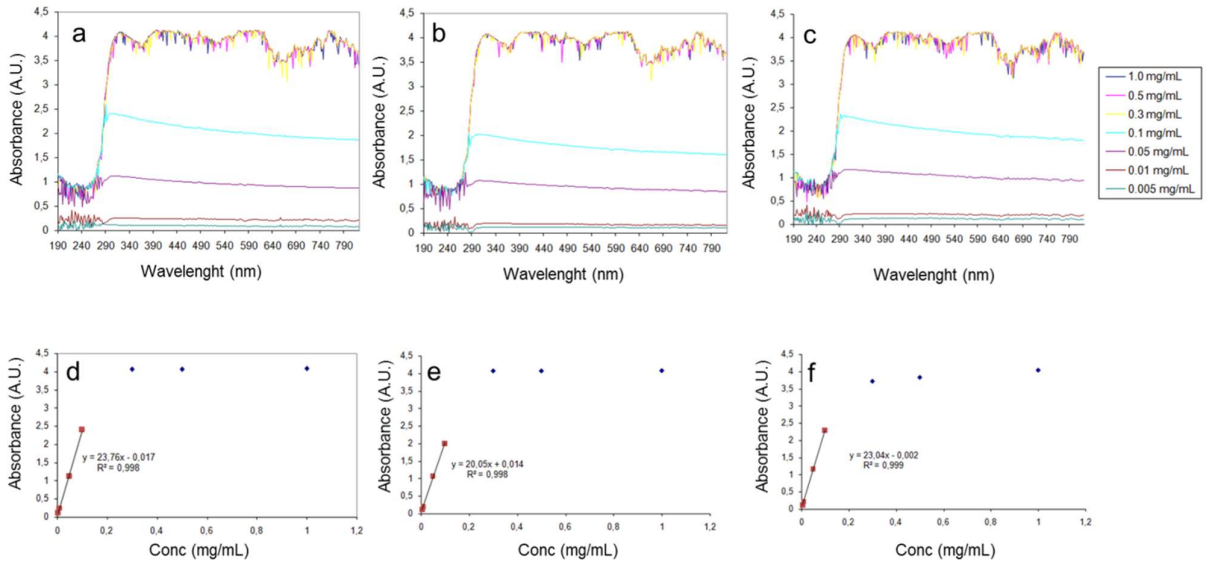


**Figure S11.** Dependence of UV-Vis absorbance on concentration of HSAG/Pyr-COOEt water suspensions HSAG/Pyr-COOEt adduct at 110°C(a), at 130°C(b) and at 160°C(c);
Linear relationship between the absorbance at 320 nm and the concentration of water suspensions of HSAG/Pyr-COOEt adducts at 110°C (d), at 130°C (e) and at 160°C (f)

In **Figure S12** are reported the UV-Vis absorbance as function of time HSAG/Pyr-COOEt water suspensions. Stability of HSAG/Pyr-COOEt suspension was verified at a concentration of 1 mg/mL, after storage for 2 hours, 5 hours, 24 hours and 1 week.

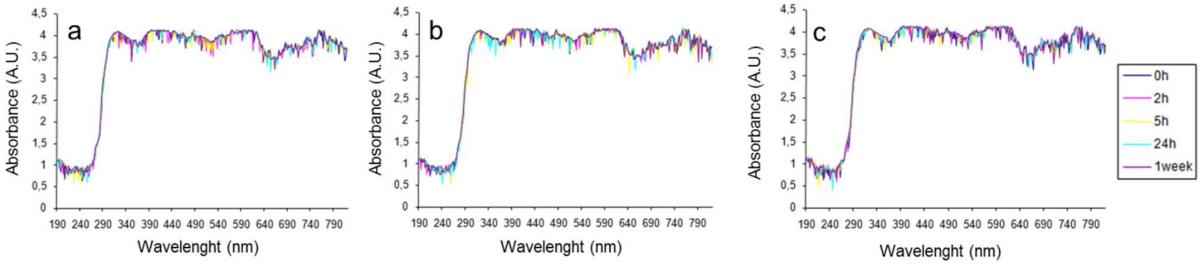


**Figure S12.** Dependence of UV-Vis absorbance on time of HSAG/Pyr-COOEt water suspensions (1 mg/mL): HSAG/Pyr-COOEt adduct at 110°C(a), at 130°C(b) and at 160°C(c).